Pulsed focused ultrasound exposures enhance locally administered gene therapy in a murine solid tumor model

Ali Ziadloo and Jianwu Xie
Molecular Imaging Lab, Department of Radiology and Imaging Sciences, Clinical Center, National Institutes of Health, 10 Center Drive, Bethesda, Maryland 20892

Victor Frenkel[a)]
Department of Biomedical Engineering, Catholic University of America, 620 Michigan Avenue, N.E., Washington, DC 20064

(Received 14 May 2012; revised 5 September 2012; accepted 21 September 2012)

Gene therapy by intratumoral injection is a promising approach for treating solid tumors. However, this approach has limited success due to insufficient distribution of gene vectors used for gene delivery. Previous studies have shown that pulsed-focused ultrasound (pFUS) can enhance both systemic and local delivery of therapeutic agents in solid tumors and other disease models. Here, murine squamous cell carcinoma flank tumors were treated with single intratumoral injection of naked tumor necrosis factor-alpha (TNF-α) plasmid, either with or without a preceding pFUS exposure. The exposures were given at 1 MHz, at a spatial average, temporal peak intensity of 2660 W cm^{-2}, using 50 ms pulses, given at a pulse repetition frequency of 1 Hz. One hundred pulses were given at individual raster points, spaced evenly over the projected surface of the tumor at a distance of 2 mm. Exposures alone had no effect on tumor growth. Significant growth inhibition was observed with injection of TNF-α plasmid, and tumor growth was further inhibited with pFUS. Improved results with pFUS correlated with larger necrotic regions in histological sections and improved distribution and penetration of fluorescent surrogate nanoparticles. Electron microscopy demonstrated enlarged gaps between cells in exposed tissue, and remote acoustic palpation showed decreases in tissue stiffness after pFUS. Combined, these results suggest pFUS effects may be reducing barriers for tissue transport and additionally lowering interstitial fluid pressure to further improve delivery and distribution of injected plasmid for greater therapeutic effects. This suggests that pFUS could potentially be beneficial for improving local gene therapy treatment of human malignancies. [http://dx.doi.org/10.1121/1.4789390]

PACS number(s): 43.80.Sh [DLM] Pages: 1827–1834

I. INTRODUCTION

Since the first human gene therapy trial in 1998, there have been over 500 gene therapy trials tracked by the NIH Recombinant Advisory Committee, where more than half of these have been intended for cancer treatment. Targets for gene therapy in cancer continue to increase with an understanding of human cancer biology and tumor-host interactions, which reinforces the close tie between the accumulation of knowledge and the potential of success for gene therapy procedures. Safe and effective treatment of cancer with gene therapy, however, still remains a major challenge for widespread clinical implementation (Gottesman, 2003).

Therapeutic genes can be delivered to solid tumors by systemic administration or direct injection. Systemic delivery has its drawbacks including the potential for toxicity to normal tissues. Sufficient and uniform delivery may also be hampered due to factors associated with the tumor microenvironment, such as heterogeneous vasculature and high interstitial fluid pressure (IFP) (Yuan, 1998; Heldin *et al.*, 2004). These obstacles may be circumvented through local administration. Indeed, a variety of clinical trials have been carried out by employing intratumoral injection. These include the use of tumor necrosis factor (TNF) related apoptosis-inducing ligand (TRAIL) for the treatment of lung cancer (Soria *et al.*, 2010), granulocyte-macrophage colony-stimulating factor (GM-CSF) for cutaneous melanoma (Mastrangelo *et al.*, 1999), and interluekin-12 (IL-12) for metastatic melanoma (Triozzi *et al.*, 2005). Despite the advantages of direct administration, this procedure still suffers from limited penetration and distribution of gene vectors (Sauthoff *et al.*, 2003; Smith *et al.*, 2011).

A number of factors in the tumor microenvironment are responsible for inhomogeneous and poor delivery of anti-cancer therapeutic agents. Structural and functional aberrations in the vasculature and extracellular matrix can impair both transvascular and interstitial transport. Tumor vasculature is abnormal in the form of large gaps between endothelial cells (rendering them leaky), non-uniform vessel distribution, and irregular microvessel size. These factors, in combination with a lack of functional lymphatics and vascular compression by the cancer cells, can contribute to high IFP, which is the hallmark of solid tumors. As a result, high IFP can reduce extravasation and limit the

[a)]Author to whom correspondence should be addressed. Also at Molecular Imaging Lab, Department of Radiology and Imaging Sciences, Clinical Center, National Institutes of Health, 10 Center Drive, Bethesda, MD 20892. Electronic mail: frenkel@cua.edu

penetration of agents in to the core of tumors (Heldin *et al.*, 2004).

Additional factors exist in the extracellular matrix (ECM) of tumors that may limit interstitial transport, and further prevent sufficient and uniform distribution of anticancer agents, especially large agents such as viral gene vectors (Wang and Yuan, 2006). The ECM is comprised of a matrix of collagen, proteoglycans, and other molecules produced and assembled by stromal and tumor cells (Mow *et al.*, 1984). McGuire *et al.* (2006) showed that greater collagen content in the ECM required higher infusion pressure in order to initiate flow in the tumor interstitium. It was also demonstrated that an inverse relationship exists between tumor content of fibrillar collagen and interstitial diffusion rates of large macromolecules (Netti *et al.*, 2000). Collagen in the ECM can physically obstruct transport, where the size of viral gene vectors, for example, can be larger than the space between the fibers (Wang and Yuan, 2006). The effects of collagen on reducing interstitial transport have indeed been established, where treatment with collagenase to chemically disrupt the fibers was shown to increase interstitial transport of antibodies (Netti *et al.*, 2000) and oncolytic viruses (McKee *et al.*, 2006). Collagen fibers also bind and stabilize glycosaminoglycan and hyaluronic acid, where these molecules can affect interstitial transport by decreasing hydraulic conductivity through the creation of resistance to water and solute transport (Netti *et al.*, 2000).

Focused ultrasound (FUS) exposures are traditionally used in continuous mode to maximize the generation of heat for tissue ablation by the process of coagulative necrosis. Today, these types of exposures are being used in the clinic for the treatment of uterine fibroids, as well as for prostate and breast tumors (Kennedy, 2005). However, by providing the exposures in pulsed mode (pFUS) using duty cycles that are typically 5% or 10%, the rate of energy deposition can be substantially lowered, where cooling can also occur between the pulses. As a result, temperature elevations may be just a few degrees Celsius (and hence non-destructive), allowing for more delicate, non-thermal mechanisms to occur (Frenkel, 2008).

pFUS exposures have demonstrated the ability to non-invasively enhance the delivery of a variety of systemically administered agents to solid tumors, including small molecules (Poff *et al.*, 2008), plasmid DNA (Dittmar *et al.*, 2005), monoclonal antibodies (Khaibullina *et al.*, 2008), and nanoparticles (Dittmar *et al.*, 2005; Frenkel *et al.*, 2006). More recently, these exposures were shown to enhance the distribution of locally administered nanoparticles in skeletal muscle (Hancock *et al.*, 2009). The manner by which this enhancement occurs is generally thought to be mediated by non-thermal mechanisms of ultrasound (e.g., acoustic cavitation and acoustic radiation forces), where these can generate effects that transiently increase the effective pore size of a tissue, and hence its permeability (Frenkel, 2008). In the present study, investigations were carried out to determine if combining pFUS exposures with intratumoral injection of plasmid DNA encoding for a therapeutic gene could lead to enhanced tumor growth inhibition in a murine solid tumor model. Additional investigations were performed in order to help elucidate the manner by which this occurred.

II. MATERIALS AND METHODS

A. Plasmid DNA

Amplification of TNF-α plasmid was performed by PCR from human genomic cDNA corresponding to the TNF-α gene with oligonucleotide primers encoding *Xba* I and *Sal* I restriction sites. The pCI-neo (Promega, Madison, WI) backbone was digested with *Xba* I and *Sal* I and the backbone and TNF-α were ligated using T4 DNA Ligase (Fermentas, Hanover, MD). The ligation mixture was transformed into DH5α chemically competent cells (Invitrogen, Carlsbad, CA). The resulting plasmid, named pCI-TNF-α, was extracted and analyzed by restriction analysis on a 2D agarose gel. Large-scale cultures of the plasmid were produced and the plasmid DNA, extracted using a High Speed Maxiprep Kit (Qiagen, Valencia, CA), and resuspended in endotoxin-free TE buffer (10 mM Tris-Cl, *p*H 7.5, 1.0 mM EDTA, <10 EU/ml). Plasmids were prepared for injection by diluting DNA to a final concentration of 1.0 μg/μl with Phosphate Buffered Saline (PBS).

B. Tumor model

A murine squamous cell carcinoma (SCCVII) cell line was used for this study. One million cells were implanted subcutaneously in the unilateral flanks of female C3H mice (25 g) as previously described (Dittmar *et al.*, 2005). For all studies, tumors were grown to a size of 250 mm^3 and then randomized into groups. All animal work was performed in compliance with institutional animal care and use committee (IACUC) guidelines, and according to an animal study protocol approved by the NIH Clinical Center ACUC.

C. Focused Ultrasound (FUS) system

A custom built, image guided, FUS system, modified from a Sonoblate® 500 (Focus Surgery, Indianapolis, IN) was used to provide all exposures. This clinical version of this device is currently being used transrectally for the ablation of prostate tumors (Kennedy, 2005). The probe possessed a spherical, concave 1 MHz therapeutic transducer (5 cm diameter; 4 cm focal length) and a co-axial 10 MHz imaging transducer (8 mm aperture). The focal zone of the therapeutic transducer was in the shape of an elongated ellipsoid, with an axial length (−3 dB) of 7.2 mm and radial diameter (−3 dB) of 1.38 mm, as determined by the manufacturer.

D. pFUS exposures

Pulsed FUS (pFUS) exposures were carried out as previously described in Frenkel *et al.* (2006). Mice were anesthetized with inhalation isofluorane (2%) during the entire exposure process. Tumors were shaved and ultrasonic coupling gel was applied to exclude trapped air bubbles. Individual mice were secured in a holder, which connected to a 3-D stage. The entire assembly was placed in a tank of degassed water (37 °C), where the mice (positioned upright) had their head above the water. This image-guided procedure used for the treatment planning was the same as the one used

for the clinical device. Employing the imaging transducer and the graphic user interface of the FUS system, the stage was used to position the mice so that the tumor to be treated was directly within the focal zone of the transducer. The beam was directed at the center of the tumor's depth (z dimension), and a rastering sequence in the x and y plane was designated in a grid pattern, with a lateral (x) and vertical (y) spacing of 2 mm between raster points.

All exposures were carried out with a spatial average, temporal peak intensity (I_{SATP}) of 2660 W cm^{-2}. The peak negative pressure was 8.95 MPa, corresponding to a mechanical index (MI) of 8.95. One hundred pulses were given at each raster point, using a pulse repetition frequency of 1 Hz, and a duty cycle of 5% (50 ms ON; 950 ms OFF). With these exposure parameters each treatment lasted 15 min.

E. Tumor growth inhibition

Mice bearing SCCVII tumors were randomized into six treatment groups (n = 5): untreated controls, saline injection alone, pFUS alone, pFUS preceding saline injection, TNF-α injection alone, and pFUS preceding TNF-α injection. All saline and TNF-α (1 μg/μl) injection volumes were 50 μl and given with a 27 [1/2] G needle following completion of the pFUS exposure (when provided). Tumor growth was monitored daily by caliper measurement, where tumor volumes were calculated as (length × $width^2$)/2. Mice were euthanized on day 7 post-treatment or when tumor diameter exceeded 2 cm.

F. Light microscopy

On day 7 of the therapeutic study, all tumors (n = 5) from the TNF-α only and the pFUS & TNF-α groups were harvested from the euthanized animals for histology. In brief, the tumors were fixed with 10% formalin, dehydrated in graded alcohol, cleared in xylene, embedded in paraffin, sectioned, and mounted on glass slides. The mounted samples were then deparaffinized in xylene, and rehydrated in graded alcohol. Finally, the samples were stained with hematoxylin-eosin (H&E), dehydrated in graded alcohol, cleared in xylene, and then cover-slipped. Slides were viewed using a microscope (Axioplan 2; Carl Zeiss MicroImaging, NY) at 100× and representative digital images were captured (Dittmar *et al.*, 2005).

G. Multispectral fluorescent imaging

Five mice were treated with pFUS and an additional five mice served as untreated controls. Immediately following the pFUS exposures 10 μl of fluorescent nanoparticles (Molecular Probes, Eugene, OR) was injected directly in to the core of the tumors using a 27 [1/2] G needle. The nanoparticles (diameter: 100 nm) were injected at a stock concentration of 10^{13} ml^{-1}, and possessed an excitation and emission spectra of 580 nm and 605 nm, respectively, 30 min later, the mice were euthanized and the skin over the tumors was removed. Whole tumor images of the fluorescent nanoparticles were captured using a Maestro multispectral imager (CRI, Cambridge, MA) as previously described (Hancock *et al.*, 2009). Images were then captured of the whole tumors. The tumors were then excised and halved, and additional images were captured. Background and autofluorescence was removed from the images using the built-in Maestro software, leaving only the positive signal produced by the nanoparticles. Bright field (grayscale) images were also captured for scaling purposes. All images were saved in digital form.

H. Transmission electron microscopy (TEM)

Three mice were treated with pFUS and tumors were immediately harvested. Three untreated (control) mice were similarly used. The tumors were fixed in glutaric dialdehyde (3% v/v) and osmium tetroxide (1% v/v) in sodium cacodylate buffer (0.1 M, *p*H 7.3), dehydrated in increasing concentrations (50%–100%) of ethanol, and cleared with propylene oxide. An interior portion of each tumor (125 mm^3) was embedded in Epon (45% agar 100 resin; 26.7% methyl nadia anhydride; 26.7% dodecenyl succinic anhydride; 1.6% benzyldimethylamine v/v). Sections from the prepared blocks were mounted on copper grids, which were then constrasted with both uranyl acetate and lead citrate. The samples were viewed with a JEOL 1230 (Tokyo, Japan) transmission electron microscope and representative digital images were captured.

I. Remote Acoustic Palpation (RAP)

In order to observe potential changes in the mechanical properties of the tumors in response to the pFUS exposures, remote acoustic palpation (RAP) was performed in four mice as previously described (Hancock *et al.*, 2009). In short, individual pulses (identical to those used in the study for treating the tumors) were given at 9 individual positions, distributed equally in the x-y plane (3 × 3) of the project surface of the tumors. Radiofrequency (RF) data (i.e., A scans) were collected immediately before and after the pulses, and a standard image processing, cross-correlation procedure was used to determine both the peak displacement produced in the tissue, and the time required for the tissue to return back to its pre-pulse, resting state. The RF data was collected using the co-axial imaging transducer of the FUS probe. Following the collection of this data, the entire tumors were treated with the pFUS exposures. The RAP procedure was then repeated and the two measured parameters were compared for pre- and post-treatment conditions.

J. Statistical analysis

A Tukey-Kramer Honestly Significant Difference (HSD) test was performed (JMP software package, Gary, NC) to determine if significant differences existed between each possible pair combination of experimental groups means of the relative growth rates of the tumors. For the acoustic palpation results, a *t* test was used to determine if changes occurred in displacement and relaxation rate in the treated tumors relative to their pretreated state. For all tests, a significant difference between individual groups was determined by a P value less than or equal to 0.05.

III. RESULTS

Tumor volumes were measured at different time points post-treatment to assess tumor growth. Monitoring of tumor volume up to day 5 post-treatment showed that tumors treated with pFUS exposures alone, intratumoral injection of saline alone, and the combination of the two, were not significantly different compared to untreated controls. However, significant growth reduction was observed for tumors receiving TNF-α only, and further significant reduction was found when these injections were preceded by pFUS [Figs. 1(a) and 1(b)].

Tumors were dissected and examined for regions of necrosis. Tumors given TNF-α injection alone had a predominance of necrosis along the surface of the tumor. Necrosis through cross-sections of the needle track was minimal and inconsistent. Tumors treated with pFUS and TNF-α demonstrated broader regions of surface necrosis as well as more diffuse patterns of necrosis radiating away from the needle track in the center of the tumor (Fig. 2).

Fluorescent nanoparticles were used as surrogates to the plasmid in order to assess the effects of pFUS on penetration and distribution of the agent into the tumor. In tumors not given pFUS exposures, signals from the fluorescent nanoparticles were observed predominantly along the surface of the tumor and cross-sectional images revealed only minimal fluorescence in the more interior regions. In contrast, tumors pre-treated with pFUS had markedly less fluorescent signals at the tumor surface. However, there were much broader and brighter regions of fluorescence in the interior of the tumors (Fig. 2).

TEM was performed to examine the effects of pFUS on the ultrastructure of the tumors. TEM showed noticeable gaps between cells in the parenchyma of tumors receiving pFUS exposures. Despite these structural changes, no evidence of damage was apparent in the tissues and all cells remained intact. These gaps, however, were not observed in the control (i.e., untreated) tumors (Fig. 3).

RAP was carried out to study the effects of pFUS on on the mechanical properties of the tumors. The results of the measurements appear in Fig. 4. All four tumors tested showed a significant decrease in the rate of relaxation of the displaced tissue following the pFUS exposures. However, no change in peak tissue displacement was observed in any of the tumors after the pFUS exposures.

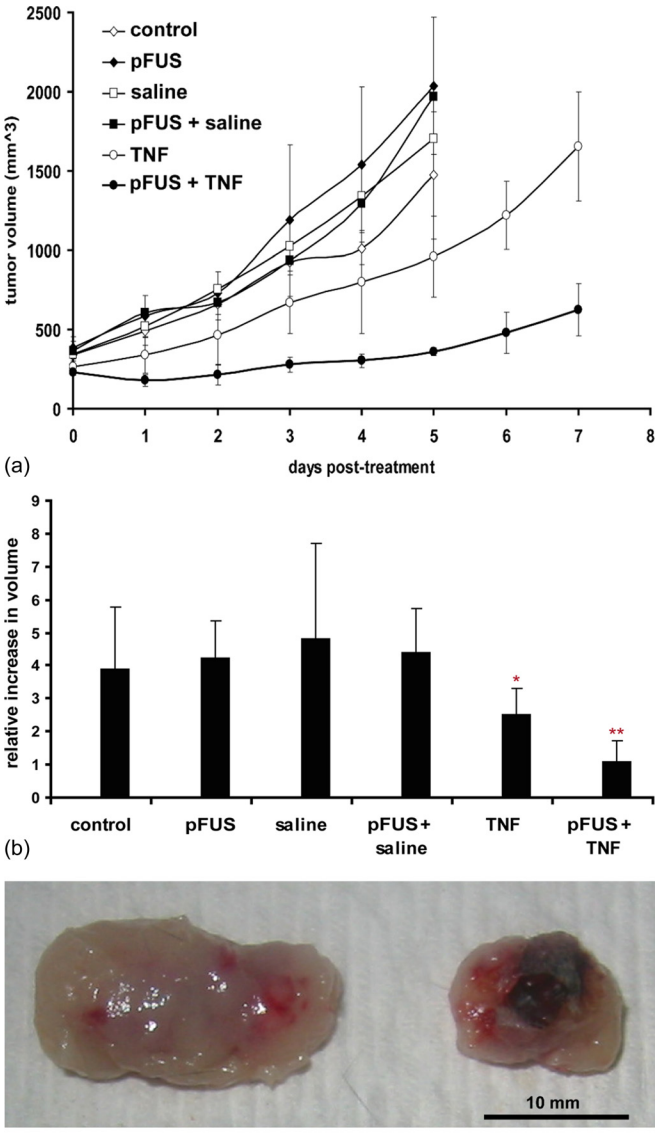

FIG. 1. (Color online) Results of the therapeutic study: (a) Tumor growth curves for the different experimental groups. (b) Relative growth rates (calculated as the ratio of the final and initial tumor volumes) for the different experimental groups ($n = 5$). pFUS exposures, injections of saline, and the combination of the two were not significantly different than the untreated controls. Tumors receiving only injections of the TNF-α plasmid grew significantly slower ($p < 0.05$), and tumors that received pFUS prior to the injections grew even slower ($p < 0.05$). (c) Representative tumors on day 5 post-treatment: left—TNF-α plasmid; right—pFUS combined with TNF-α plasmid.

IV. DISCUSSION

pFUS exposures similar to those employed in the present study have been used to non-invasively and non-destructively enhance the delivery of a variety of systemically administered agents in murine solid tumors including plasmid DNA (Dittmar *et al.*, 2005), small molecules (Poff *et al.*, 2008), nanoparticles (Frenkel *et al.*, 2006), and monoclonal antibodies (Khaibullina *et al.*, 2008). More recently, in a study in the murine skeletal muscle, the same exposures were shown to enhance the delivery of both systemically and locally administered nanoparticles (Hancock *et al.*, 2009). The present study is the first to demonstrate that these exposures can enhance the delivery of a locally administered agent in a solid tumor model. When substituting these nanoparticles with plasmid DNA encoding for the cytokine TNF-α, enlarged regions of necrosis were observed in the tumors when the injections were preceded by the pFUS exposures, compared to the TNF-α plasmid injections alone. These effects were also found to coincide with significantly lower tumor growth rates.

Naked plasmid DNA has been shown to be an attractive non-viral alternative for gene transfer due to very low transfection at distant sites and relatively limited immune response, even following multiple injections (Wolff and Budker, 2005). Direct injections of both viral and non-viral gene vectors into tumors can be advantageous in order to

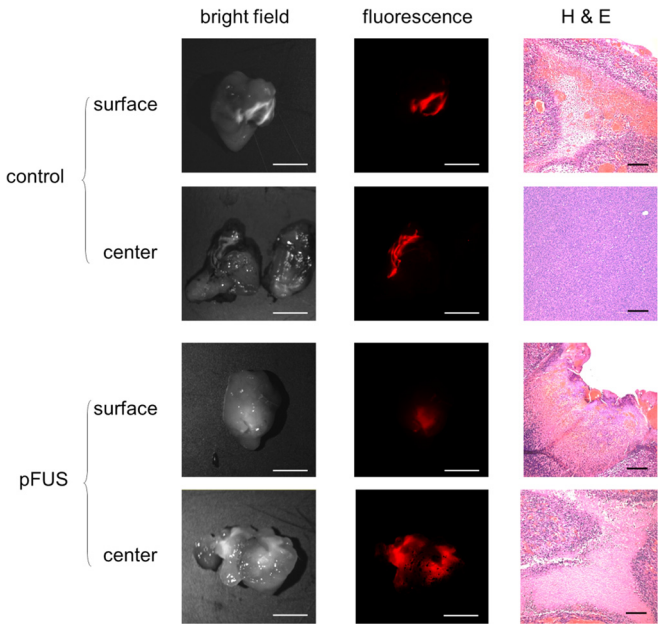

FIG. 2. (Color online) Representative images of whole tumors treated and untreated (control) with pFUS. The two columns on the left show images captured in whole tumors, both intact (surface) and halved (center). The treated tumor shows more nanoparticles to have penetrated in to the center of the tumor; however, these appear to remain closer to the surface in the untreated tumor (scale bar = 5 mm). The column on the right shows images captured with bright field microscopy of tumor sections stained with H&E (scale bar = 50 μm). The treated tumor shows more extensive necrosis at the surface as well as in the more interior region.

limit the expression of the gene products to a targeted region. This procedure also precludes the need to overcome the obstacle of limited extravasation, which is especially important for large agents such as viral vectors (Wang and Yuan, 2006). Systemic administration of naked DNA is also not recommended due to the presence of DNAase in the plasma (Borchard, 2001; Mao *et al.*, 2001). Despite these advantages of intratumoral injections, this type of treatment can also be less than effective because of limited distribution of the injected agents (Sauthoff *et al.*, 2003; Jia and Zhou, 2005; Smith *et al.*, 2011; Zhao *et al.*, 2011). In the present study, broader regions of necrosis were observed in the tumors treated with pFUS compared to the untreated ones, which correlated well with distributions of fluorescently labeled nanoparticles. This suggests that pFUS exposures could have enhanced the distribution of injected TNF-α plasmid in the tumors. The same pFUS exposures in murine skeletal muscle similarly showed improved distribution of nanoparticles that were injected directly into the tissue after the exposures (Hancock *et al.*, 2009).

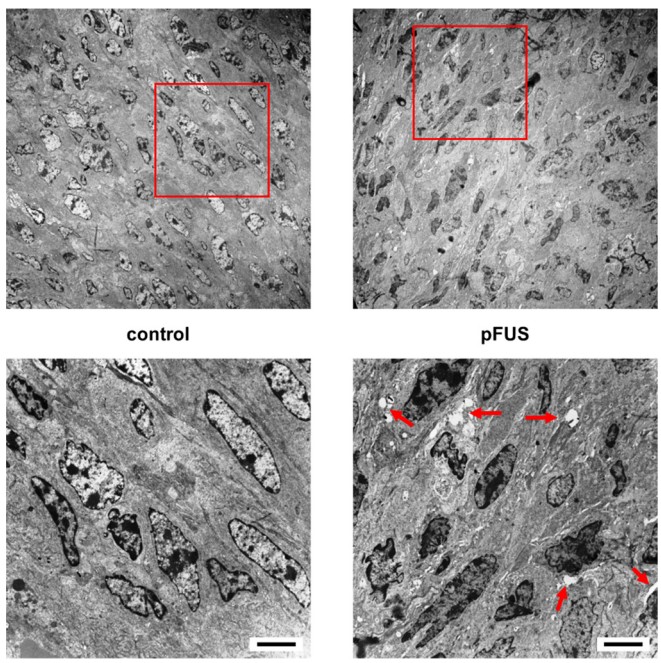

FIG. 3. (Color online) Representative transmission electron micrographs of control and pFUS treated tumors. Bottom images are expanded from boxes in top images. Tumors exposed to pFUS showed pervasive widening of intercellular spaces (arrows) between cells in the parenchyma, which were absent in the untreated tumors (scale bar = 5 μm).

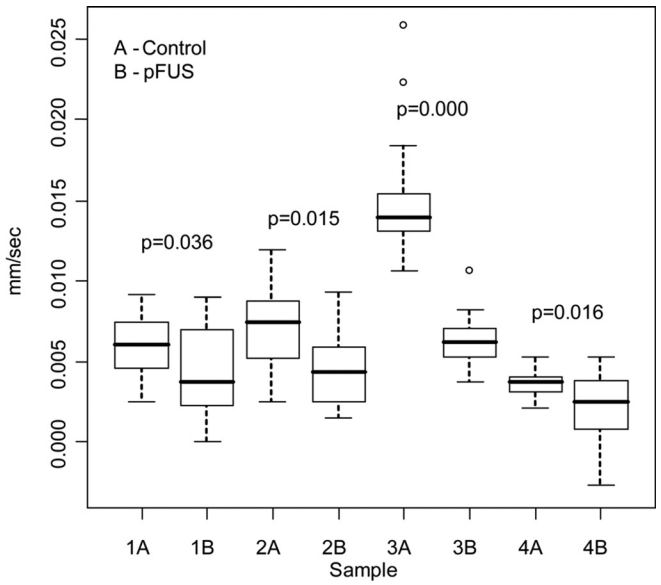

FIG. 4. Comparison of relaxation rates in four individual tumors before (control) and after pFUS exposures. Measurements (n = 9) were taken for a single FUS pulse using RAP. Significant decreases were found in relaxation rates in all tumors after the pFUS exposures ($p < 0.05$). The central (dark) line is the median, the edges of the box are the 25th (Q1) and 75th (Q3) percentiles, and the outer lines extend to the most extreme data points (minimum and maximum) that are not outliers. Data points are considered outliers, designated by open circles, if they are smaller than $Q1 - 1.5 \times (Q3 - Q1)$ or larger than $Q3 + 1.5 \times (Q3 - Q1)$.

Observations with transmission electron microscopy (TEM) showed enlarged intercellular gaps between cells in regions of the tumors exposed to pFUS, in comparison to similar regions in the untreated tumors where these gaps were not present. It is not unreasonable to suggest that these gaps increased the effective pore size of the tissue allowing for enhanced distribution of the injected agents and an improved therapeutic effect. Hancock *et al.* (2009) also showed enlarged gaps between muscle fibers, suggesting that these enabled improved distribution of the agents administered into those tissues. While the relationship between effective pore size and distribution appears to be straightforward in normal tissues such as the muscle, the relationship may be more complex in solid tumors due to some of the unique features of tumor microenvironment.

Two of the major factors in the tumor microenvironment limiting adequate and uniform delivery of therapeutic agents are high interstitial fluid pressures (IFP) (Boucher *et al.*, 1990) and fibrillar collagen in the extracellular matrix (Wang and Yuan, 2006). McKee *et al.* (2006), for example, demonstrated that by altering the collagen network with collagenase in a high collagen tumor model, they could enhance the distribution of a locally administered oncolytic virus, and consequently increase its therapeutic efficacy. Head and neck squamous cell carcinoma (HNSCC) tumors, such as those used in the present study, are known to possess relatively low amounts of collagen in the ECM due to overexpression of different colleganases (Werner *et al.*, 2002), where preliminary observations (data not shown here) when staining for collagen did appear to support this. The pFUS exposures used in the skeletal muscle were shown to disrupt collagen in the ECM, in addition to opening up gaps between the muscle fiber bundles (Hancock *et al.*, 2009). Presumably, disruption of collagen in the ECM of the tumors with pFUS could have improved the distribution of the injected plasmid DNA.

The transfer of momentum from a traveling ultrasonic beam to a reflecting or absorbing body results in a force, known as an acoustic radiation force. These unidirectional forces produced by FUS pulses can generate displacements in tissues on the order of tens to hundreds of microns (Nightingale *et al.*, 2001) that can be easily measured ultrasonically. This technique is often known as remote acoustic palpation (RAP), or, if used to construct images, acoustic radiation force imaging (ARFI). Changes in the mechanical properties can be detected with RAP. In one study, for example, RAP was used to validate the formation of thermal ablative lesions produce by continuous FUS exposures. Displacement after the lesions were formed were found to be significantly lower compared to those prior to the treatments; apparently due to the denaturing of the proteins that made the tissue noticeably stiffer (Lizzi *et al.*, 2003).

In the present study, RAP was used to determine if changes could potentially be occurring in the mechanical properties of the tumors as a result of the pFUS exposures. Although changes in peak displacements were not observed, significant increases in the time required for the tissue to return back to its initial, pre-treatment state was found in all the treated tumors. Previous studies in a variety of tumors models, including HNSCC, have shown that pFUS exposures do not cause damage to the tissue (Dittmar *et al.*, 2005; Frenkel *et al.*, 2006; Khaibullina *et al.*, 2008). The increase in the relaxation time in the treated tumors, which essentially indicates a reduction in tissue elasticity, must have then occurred from a decrease in the amount of fluid in the tumors.

Although the data collected in the present study does not allow us to present a definitive explanation for the observed enhancing effects of the pFUS exposures, we can still attempt to summarize the results in the following logical manner. In addition to creating the structural effects that lead to an increase in the effective pore size of the tissue, and subsequent enhancement in the distribution of the agent (Fig. 5), these enlarged spaces between the cells may have also improved the hydraulic conductivity of the tissue (McGuire *et al.*, 2006). As a result, improved fluid flow may have occurred from regions of high pressure that are normally found in the tumor cores to the periphery, where the pressure is known to be lower (Boucher *et al.*, 2000). This would have enabled more fluid to be taken up by functional

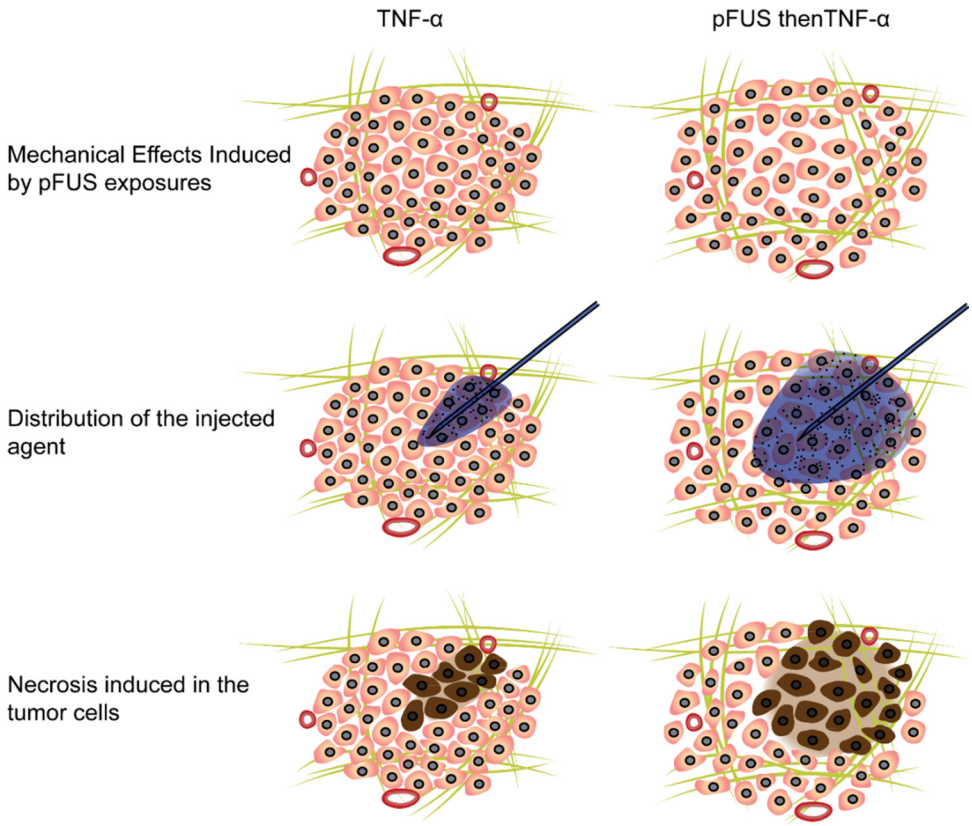

FIG. 5. (Color online) Schematic representation of the proposed manner by which the pFUS exposures enhanced the therapeutic effects of the TNF-α plasmid injections. (Top) pFUS exposures create mechanical effects in the form of enlarged gaps between the parenchymal cells in the tumors; (middle) these effects allow for better penetration and distribution of the injected agent; (bottom) as a result, a larger region of necrosis within the tumors is created, which ultimately leads to slower tumor growth rates. Note, enlarged gaps between cells created by the pFUS exposures may also be increasing hydraulic conductivity in the interstitium, leading to lower IFP, and further contributing to improved bioavailability of the injected agent.

vessels; also found in greater abundance in the periphery (Jain, 1990, 1997). This subsequently would have lowered the overall IFP in the tumors, and ultimately contributed to better penetration and distribution of the injected agent.

To investigate the manner by which gaps are generated in the tissue by pFUS, a novel mechanism was recently proposed based on the large displacements (i.e., hundreds of microns) produced by the radiation forces that occur during each FUS pulse (Hancock *et al.*, 2009). One of the unique features of these displacements is the large gradient that occurs at the edge of the focus, between regions of tissue that are actively being displaced (in the focal zone) and those that are not (immediately adjacent to the focal zone). Simulations of the exposures showed that this non-uniform movement being produced in the tissue generates substantial shear strain in this transition zone that could very reasonably have produced the large gaps in tissue. In murine muscle, these effects were found to be non-destructive, as well as reversible, where the tissue reverted back to its initial state over a period of 2 to 3 days (Hancock *et al.*, 2009). Both these features, especially reversibility, would be extremely important for the treatment of tumors, and is one among the many directions that should be addressed in future studies for the development of this procedure.

It is possible that the generation of heat and acoustic cavitation may have also contributed as mechanisms for inducing the effects presented in this study. More detailed investigations on their contributions for similar purposes (i.e., enhancing permeability) were recently carried out, where the evidence collected appears to point to a more minor or even insignificant role for either mechanism (O'Neill *et al.*, 2009; Hancock *et al.*, 2009).

V. CONCLUSIONS

In conclusion, we determined that intratumoral injection of TNF-α plasmid when preceded by pFUS exposures results in enhanced tumor growth inhibition compared to TNF-α injections alone. We showed that the increase in efficacy most likely derives from non-destructive mechanical effects produced by the exposures (i.e., gaps between the cells), which can increase the effective pore size of the tissue for improved distribution of the agent. These gaps may also be improving hydraulic conductivity within the interstitium, lowering IFP, and hence further improving bioavailability of the injected agents. The results of this study are not only applicable to naked plasmid but may also have implications for viral gene delivery, nanotechnology platforms, and traditional chemotherapy; all of which face tumor delivery barriers (Wang and Yuan, 2006). Ultimately, combining pFUS with cancer therapeutics may be beneficial in the local treatment of many unresectable human malignancies, including HNSCC and melanoma.

ACKNOWLEDGMENTS

The authors would like to especially thank Dr. B. O'Neill of Methodist Hospital in Houston for his contributions to the RAP data, and K Nagashima of the National Cancer Institute for his assistance with the electron microscopy. We would also like to express our gratitude to Dr. Yves Boucher of Harvard University for his thoughtful insights on core topics related to this study. This research was supported in part by the intra-mural research program of the Clinical Center, National Institutes of Health (NIH).

Borchard, G. (**2001**). "Chitosans for gene delivery," Adv. Drug Delivery Rev. **52**, 145–150.

Boucher, P. D., Ostruszka, L. J., and Shewach, D. S. (**2000**). "Synergistic enhancement of herpes simplex virus thymidine kinase/ganciclovir-mediated cytoxicity by hydroxyurea," Cancer Res. **60**, 1631–1636.

Boucher, Y., Baxter, L. T., and Jain, R. K. (**1990**). "Interstitial pressure gradients in tissue-isolated and subcutaneous tumors: Implications for therapy," Cancer Res. **50**, 4478–4484.

Dittmar, K. M., Xie, J., Hunter, F., Trimble, C., Bur, M., Frenkel, V., and Li, K. C. (**2005**). "Pulsed high-intensity focused ultrasound enhances systemic administration of naked DNA in squamous cell carcinoma model: Initial experience," Radiology **235**, 541–546.

Frenkel, V. (**2008**). "Ultrasound mediated delivery of drugs and genes to solid tumors," Adv. Drug Delivery Rev. **60**, 1193–1208.

Frenkel, V., Etherington, A., Greene, M., Quijano, J., Xie, J., Hunter, F., Dromi, S., and Li, K. C. (**2006**). "Delivery of liposomal doxorubicin (Doxil) in a breast cancer tumor model: Investigation of potential enhancement by pulsed-high intensity focused ultrasound exposure," Acad. Radiol. **13**, 469–479.

Gottesman, M. M. (**2003**). "Cancer gene therapy: An awkward adolescence," Cancer Gene Ther. **10**, 501–508.

Hancock, H. A., Smith, L. H., Cuesta, J., Durrani, A. K., Angstadt, M., Palmeri, M. L., Kimmel, E., and Frenkel, V. (**2009**). "Investigations into pulsed high-intensity focused ultrasound-enhanced delivery: Preliminary evidence for a novel mechanism," Ultrasound Med. Biol. **35**, 1722–1736.

Heldin, C. H., Rubin, K., Pietras, K., and Ostman, A. (**2004**). "High interstitial fluid pressure—An obstacle in cancer therapy," Nat. Rev. Cancer **4**, 806–813.

Jain, R. K. (**1990**). "Vascular and interstitial barriers to delivery of therapeutic agents in tumors," Cancer Metastasis Rev. **9**, 253–266.

Jain, R. K. (**1997**). "Delivery of molecular and cellular medicine to solid tumors," Adv. Drug Delivery Rev. **26**, 71–90.

Jia, W., and Zhou, Q. (**2005**). "Viral vectors for cancer gene therapy: Viral dissemination and tumor targeting," Curr. Gene Ther. **5**, 133–142.

Kennedy, J. E. (**2005**). "High-intensity focused ultrasound in the treatment of solid tumours," Nat. Rev. Cancer **5**, 321–327.

Khaibullina, A., Jang, B. S., Sun, H., Le, N., Yu, S., Frenkel, V., Carrasquillo, J. A., Pastan, I., Li, K. C., and Paik, C. H. (**2008**). "Pulsed high-intensity focused ultrasound enhances uptake of radiolabeled monoclonal antibody to human epidermoid tumor in nude mice," J. Nucl. Med. **49**, 295–302.

Lizzi, F. L., Muratore, R., Deng, C. X., Ketterling, J. A., Alam, S. K., Mikaelian, S., and Kalisz, A. (**2003**). "Radiation-force technique to monitor lesions during ultrasonic therapy," Ultrasound Med. Biol. **29**, 1593–1605.

Mao, H. Q., Roy, K., Troung-Le, V. L., Janes, K. A., Lin, K. Y., Wang, Y., August, J. T., and Leong, K. W. (**2001**). "Chitosan-DNA nanoparticles as gene carriers: Synthesis, characterization and transfection efficiency," J. Control Release **70**, 399–421.

Mastrangelo, M. J., Maguire, H. C., Jr., Eisenlohr, L. C., Laughlin, C. E., Monken, C. E., McCue, P. A., Kovatich, A. J., and Lattime, E. C. (**1999**). "Intratumoral recombinant GM-CSF-encoding virus as gene therapy in patients with cutaneous melanoma," Cancer Gene Ther. **6**, 409–422.

McGuire, S., Zaharoff, D., and Yuan, F. (**2006**). "Nonlinear dependence of hydraulic conductivity on tissue deformation during intratumoral infusion," Ann. Biomed. Eng. **34**, 1173–1181.

McKee, T. D., Grandi, P., Mok, W., Alexandrakis, G., Insin, N., Zimmer, J. P., Bawendi, M. G., Boucher, Y., Breakefield, X. O., and Jain, R. K. (**2006**). "Degradation of fibrillar collagen in a human melanoma xenograft improves the efficacy of an oncolytic herpes simplex virus vector," Cancer Res. **66**, 2509–2513.

Mow, V. C., Mak, A. F., Lai, W. M., Rosenberg, L. C., and Tang, L. H. (**1984**). "Viscoelastic properties of proteoglycan subunits and aggregates in varying solution concentrations," J. Biomech. **17**, 325–338.

Netti, P. A., Berk, D. A., Swartz, M. A., Grodzinsky, A. J., and Jain, R. K. (**2000**). "Role of extracellular matrix assembly in interstitial transport in solid tumors," Cancer Res. **60**, 2497–2503.

Nightingale, K. R., Palmeri, M. L., Nightingale, R. W., and Trahey, G. E. (**2001**). "On the feasibility of remote palpation using acoustic radiation force," J. Acoust. Soc. Am. **110**, 625–634.
O'Neill, B. E., Vo, H., Angstadt, M., Li, K. C., Quinn, T. and Frenkel, V. (**2009**). "Pulsed high intensity focused ultrasouond mediated nanoparticle delivery: Mechanisms and efficacy in murine muscle," Ultrasound Med. Biol. **35**, 416–424.
Poff, J. A., Allen, C. T., Traughber, B., Colunga, A., Xie, J., Chen, Z., Wood, B. J., Van Waes, C., Li, K. C., and Frenkel, V. (**2008**). "Pulsed high-intensity focused ultrasound enhances apoptosis and growth inhibition of squamous cell carcinoma xenografts with proteasome inhibitor bortezomib," Radiology **248**, 485–491.
Sauthoff, H., Hu, J., Maca, C., Goldman, M., Heitner, S., Yee, H., Pipiya, T., Rom, W. N., and Hay, J. G. (**2003**). "Intratumoral spread of wild-type adenovirus is limited after local injection of human xenograft tumors: Virus persists and spreads systemically at late time points," Human Gene Ther. **14**, 425–433.
Smith, E., Breznik, J., and Lichty, B. D. (**2011**). "Strategies to enhance viral penetration of solid tumors," Human Gene Ther. **22**, 1053–1060.
Soria, J. C., Smit, E., Khayat, D., Besse, B., Yang, X., Hsu, C. P., Reese, D., Wiezorek, J., and Blackhall, F. (**2010**). "Phase 1b study of dulanermin (recombinant human Apo2L/TRAIL) in combination with paclitaxel, carboplatin, and bevacizumab in patients with advanced non-squamous non-small-cell lung cancer," J. Clin. Oncol. **28**, 1527–1533.
Triozzi, P. L., Strong, T. V., Bucy, R. P., Allen, K. O., Carlisle, R. R., Moore, S. E., Lobuglio, A. F., and Conry, R. M. (**2005**). "Intratumoral administration of a recombinant canarypox virus expressing interleukin 12 in patients with metastatic melanoma," Human Gene Ther. **16**, 91–100.
Wang, Y., and Yuan, F. (**2006**). "Delivery of viral vectors to tumor cells: Extracellular transport, systemic distribution, and strategies for improvement," Ann. Biomed. Eng. **34**, 114–127.
Werner, J. A., Rathcke, I. O., and Mandic, R. (**2002**). "The role of matrix metalloproteinases in squamous cell carcinomas of the head and neck," Clin. Exp. Metastasis **19**, 275–282.
Wolff, J. A., and Budker, V. (**2005**). "The mechanism of naked DNA uptake and expression," Adv. Genet **54**, 3–20.
Yuan, F. (**1998**). "Transvascular drug delivery in solid tumors," Seminars Radiat. Oncol. **8**, 164–175.
Zhao, L., Wu, J., Zhou, H., Yuan, A., Zhang, X., Xu, F., and Hu, Y. (**2011**). "Local gene delivery for cancer therapy," Curr Gene Ther. **11**, 423–432.